Journal of Applied Polymer Science

Nafion-115/aromatic poly(etherimide) with isopropylidene groups/ imidazole membranes for polymer fuel cells

Agnieszka Iwan,[1] Marek Malinowski,[1] Andrzej Sikora,[1] Igor Tazbir,[1] Grzegorz Pasciak,[1] Eugenia Grabiec[2]

[1]Division of Electrotechnology and Materials Science, Electrotechnical Institute, M. Sklodowskiej-Curie 55/61 Str. 50-369 Wrocław, Poland

[2]Center of Polymer and Carbon Materials, Polish Academy of Science, 34 M. Sklodowska-Curie Str. 41-819 Zabrze, Poland

Correspondence to: A. Iwan (E-mail: a.iwan@iel.wroc.pl)

ABSTRACT: Proton exchange membrane fuel cells (PEMFCs) with Pt/C gas diffusion electrodes and graphite single-serpentine monopolar plates were constructed based on an aromatic poly(etherimide) with isopropylidene groups (PI)/imidazole (Im) and a popular Nafion-115 matrix. The electrochemical properties of PEMFCs were tested at 25 and 60°C. The maximum power density of 171 mW/cm^2 and the maximum current density of 484 mA/cm^2 were detected for Nafion-115/PI membrane. For both constructed PEMFCs the efficiency at 0.6 V was found about 41%. Immersion of Nafion-115 in PI or PI/Im increased the thermal stability and mechanical properties of membranes. Thermal, mechanical properties and morphology of membranes were characterized by TGA, and AFM techniques including force spectroscopy. Interactions between the components in composite membranes were established by FT-IR. © 2015 Wiley Periodicals, Inc. J. Appl. Polym. Sci. **2015**, *132*, 42436.

KEYWORDS: batteries and fuel cells; electrochemistry; polyimides

Received 13 February 2015; accepted 29 April 2015

DOI: 10.1002/app.42436

INTRODUCTION

Aromatic polyimides are one of the most important classes of high-performance polymers. They exhibit good mechanical, thermal, and optical properties for aerospace industries, optical and electrical devices or films and membranes.[1–3] Taking into consideration their chemical structure, aromatic polyimides can be divided onto five- and six-membered ring polyimides. Mainly, six-membered ring polyimides are investigated in high temperature (HT) polymer fuel cells (PEMFCs) because of the better stability in fuel cell environment than five-membered ring polyimides.[1–16]

Low temperature (LT), Nafion membrane-based PEMFCs are modified by various inorganic (ZrP, SiO_2, TiO_2, BPO_4, H_3PO_4, $Sn_{0,95}Al_{0,05}P_2O_7$-P_xO_y or $CsHSO_4$[17–25] or organic additives (imidazole, triazole, diethyl amine, triethylamine, polybenzimidazoles (PBI), vinylbenzyl substituted PBI, different salt forms of the Nafion ionomer, ionic liquid cation 1-butyl-3-methylimidazolium or/and phosphoric acid.[21,26–39]

PEMFCs based mainly on sulfonated six-membered ring polyimides have been reported; however, has no proton conductivity in the absence of water, likely as Nafion.[1,2,4,5] Some of the scientists propose applied imidazole to polyimide membrane into direction to improve their conductivity.[1,5,14,16] For example, Pu *et al.*[5] studied proton conductivity of PI/H_3PO_4/Im blends and showed the increase of proton conductivity along with increasing temperature and content of H_3PO_4 or Im. However, authors not investigated PEMFCs based on polyimide obtained from 4,4′-oxydiphthalic anhydride and 4,4′-diaminodiphenyl ether. Authors conclude that it would be possible significantly increase the operating temperature of PEMFCs by replacing water with imidazole as proton solvent in the PI membrane.[5] Pu *et al.*[16] studies also anhydrous proton conducting of membrane based on 2-undecylimidazole and sulfonated six-membered ring polyimide. The addition of Im derivatives in PI improved the chemical oxidation stability of the composite membranes, even better than of pure PI, and increases along with increase the content of Im and reaches the proton conductivity 10^{-3} S/cm at 180°C under the anhydrous condition.

For PEMFCs, many investigations are still carried out including such important aspects as: (i) synthesis of polymers to be used as electrolytes in PEMFCs, (ii) optimization of the construction of PEMFCs via modification of the electrodes, bipolar plates and engineering processes, and (iii) evaluation of the single PEMFC and finally the entire stack.[1–3,40–49]

In our previous work, we have investigated influence of polybenzimidazole ($PBICF_3$),[50] imidazole and 2,2′-bis(4-

aminophenyl)−5,5′-bibenzimidazole (BAPBI)[51] on the electrochemical properties of Nafion-115 membrane. In the last decade acid-base blend membranes consisting of polymer with sulfonic groups and a basic compound with N-heterocycle groups are one of the most promising directions for development of PEMFCs.[33,36,52,53]

Water transport phenomena are important with respect to proper description of polymer fuel cells. The significance of this issue results from the principle of fuel cell operation that leads to the production of water and also from the connection between the magnitude of the membrane water uptake (WU) and its ionic conductivity. Nafion membrane conductivity is strongly correlated with temperature. It can significantly drop with sudden loss of water molecules in the electrolyte. This can especially happen in the case of low-temperature PEMFCs if the temperature is close to 100°C. First of all, this issue is related to the anode that has to be efficiently humidified and pressurized during fuel cell operation because the rate of water back diffusion produced at the cathode side might be insufficient. On the other hand, there are many, already mentioned, advantages of fuel cell operation at high temperatures. Thus, this work aims at mitigating the membrane conductivity dependence on WU.

It is known that imidazole proton conductors are used as water replacement solvents[1,54,55] and have also been attached to polymer backbone to replace the acid/water complex in PEMFCs.[56] The melting temperature of imidazole is approximately 90°C higher than that of water at ambient pressure.[5] It was found that heterocycles such as imidazole, triazole and pyrazole are promising in avoiding strong solvent effects and acts like water as proton donor and acceptor in the proton conduction process.[5]

The modern approach is to substitute pristine, water-based membrane, for a composite obtained by the application of PI, and PI/Im modifiers. The fundamental idea is to incorporate PI and PI/Im in the membrane structure in order to prevent additives from being removed by liquid water during fuel cell operation. Acid-base interactions with regard to fuel cell operation at elevated temperatures are, therefore, the main topic of interest in this work. These results motivate us to investigate the influence of Im on the proton conductivity of PEMFCs based on Nafion/PI membrane.

Additionally, in this work, we showed that five-ring PI are suitable to be applied as modifier of Nafion membrane, while flexible PI membranes are not adequate for PEMFC application taking into consideration the fact that their conductivity is very low.

In this work, PEMFCs based on Nafion-115 and aromatic poly(-etherimide) with isopropylidene groups (PI) were constructed and characterized in details. Electrochemical properties of single PEMFCs with PI were analyzed by electrochemical impedance spectroscopy, polarization curves, cyclic voltammetry and linear sweep voltammetry taking into account the temperature used (25 and 60°C) and the presence of additional doping compound that is, imidazole. Morphology and mechanical properties of membranes were analyzed by AFM method, while interactions between Nafion-115 and PI and Im were studied by FT-IR. In our knowledge this is the first example of modification of Nafion membrane properties by immersion in five-membered ring polyimide. Finally, electrochemical properties obtained in this work for Nafion-115/PI were compared with Nafion-115/Im, Nafion-115/BAPBI and Nafion-115/PBICF$_3$ described in details in our previous studies.[50,51] We have discovered that applying PI in Nafion-115 membrane caused the increase of the maximum power density (171 mW/cm^2 at 60°C) in comparison to other investigated by us Nafion-115 membranes.[50,51]

Table I. Thermal Stability of Investigated Membranes by TGA Method

Code	$T_{5\%}$ (°C)[a]	$T_{10\%}$ (°C)[a]	$T_{20\%}$ (°C)[a]	T_p (°C)[b]	T_p (°C)[b]	T_p (°C)[b]
Nafion-115-PI	328	354	399	364	458	–
Nafion-115-PI-Im	327	354	398	366	458	–
Nafion-115[51]	288	350	431	338	447	502
Nafion-115/Im[51]	330	357	398	369	455	–

[a] $T_{5\%}$, $T_{10\%}$, and $T_{25\%}$: temperatures at 5, 10, and 20% weight loss, respectively.
[b] Temperatures at which the maximum rate of weight loss was observed according to DTG curves.

EXPERIMENTAL

Materials

Nafion-115 film was purchased from Quintech Brennstoffzellen Technologie. Imidazole (Im) and *N*,*N*-dimethylacetamide (DMA) were obtained from Aldrich and used as received.

Aromatic poly(etherimide) with isopropylidene groups (PI) was obtained from 4,4′-(hexafluoroisopropylidene) diphthalic anhydride and 4,4′-(4,4′-isopropylidene-diphenyl-1,1′-diyldioxy)dianiline in NMP solution according to the synthesis described in Ref. 57.

Preparation of Nafion-115/PI and Nafion-115/PI/Im Membranes

In the first step, Nafion-115 membrane was purified by boiling in deionized water for 1 h. Next, Nafion-115 membranes were dipped for 15 min into PI or PI/Im DMA solution (0.1% solution), and next dried at temperature of 105°C for 3 min. This procedure was repeated four times. In the third step, all membranes were cleaned by boiling in deionized water for 1 h and then rinsed in 3.75% H_2O_2 for an hour and finally activated in boiling 0.2*M* H_2SO_4 solution during 1 h. All membranes were also rinsed several times in fresh distilled water to remove any residual contaminants.

Construction of Single PEMFCs

Single PEMFCs with area of 1 cm^2 were constructed based on prepared membranes, commercial gas diffusion electrodes (SLGDE 0.5 mg cm^{-2}, FuelCellsEtc) and graphite single-serpentine plates. All fuel cells were constructed by pressing of membranes and electrodes at temperature of 100°C for 5 min under 30 bars of pressure.

Characterizations

Particular fuel cells were investigated using commercial 1 cm^2 testing fuel cell fixture (Pragma Industries) with graphite

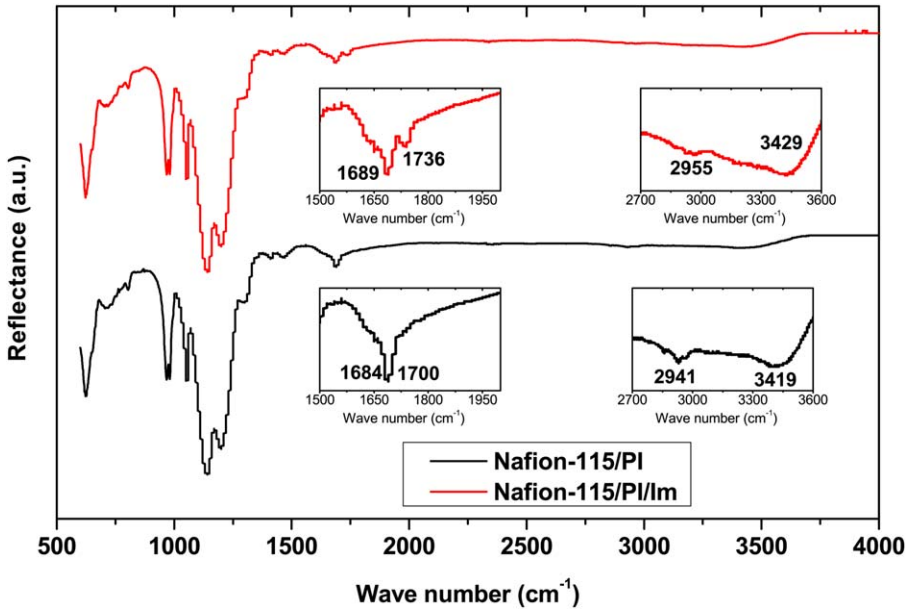

Figure 1. FTIR spectra of Nafion-115/PI and Nafion-115/PI/Im membranes. [Color figure can be viewed in the online issue, which is available at wileyonlinelibrary.com.]

single-serpentine monopolar plates. The research was carried out *in situ*, delivering to the measurement cell, reactant or inert gases depending on the method of used evaluation. Electrochemical properties of PEMFCs were investigated by polarization curve (V-J), electrochemical impedance spectroscopy (EIS), cyclic voltammetry (CV), and linear sweep voltammetry (LSV). The following equipment was used in order to perform above mentioned experiments: ZS electronic load (H&H), impedance/gain-phase analyzer SI 1260 (Solartron Analytical), SI 1287 electrochemical interface potentiostat/galwanostat (Solartron Analytical) and dedicated computer programs.

Polarization curve was performed using the configuration of hydrogen and air supplying with flow rate of 60 and 80 mL/min, respectively, under the atmospheric pressure and 90% of relative humidity. These characteristics were done in voltage mode in 60 s from the open circuit voltage to 0.25 V. Electrochemical impedance spectroscopy was performed in the frequency range from 40 kHz to 0.1 Hz using the same gaseous supplying as in V-J method. Cyclic voltammetry and linear sweep voltammetry were utilized as other measurement techniques due to which hydrogen was fed with flow rate of 50 mL/min, under the atmospheric pressure to the anode acting as counter and reference electrode while argon with the same flow rate and pressure was delivered to the second electrode being the working electrode. These measurements were taken at steady-state condition applying low scan rate of 10 mV/s.

Infrared spectra of the membranes were acquired on a Nicolet 5700 (ThermoElectron) in the range of 4000–400 cm^{-1} at a resolution of 2 cm^{-1} and for accumulated 32 scans.

Thermogravimetric analyses (TGA) and DTG were performed on a Mettler-Toledo AG apparatus at a heating rate of 10°C/min under nitrogen.

The surface morphology investigations of the membranes were performed in air using a commercial Innova AFM system from Bruker (former Veeco). Topography imaging was performed using tapping mode with phase imaging feature. The NSG30 probes

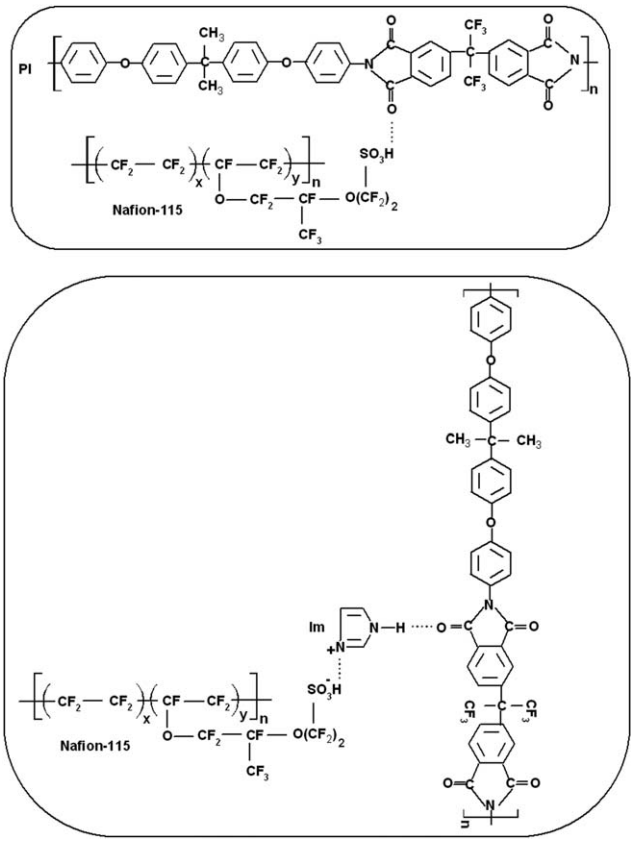

Figure 2. Possible interactions between Nafion-115/PI and Nafion-115/PI/Im.

Table II. The Surface Parameters of Investigated Membranes

	Surface statistics[a]				
Code	S_a (nm)]	S_q (nm)	S_{sk}	S_{ku}	S_{dr} (%)
Nafion-115/PI	0.5581	0.7001	0.1445	2.9646	0.891
Nafion-115/PI/Im	0.6932	0.8430	0.2894	2.5029	0.432
Nafion-115[51]	1.2021	1.5789	0.1858	4.8332	6.537
Nafion-115-Im[51]	0.3279	0.4502	0.5294	7.2920	2.787

[a] Values calculated for scanning field 300 × 300 nm^2.

from NT-MDT (k = 22–100 N/m, f_{res} = 240–440 kHz, r_{tip} = 6 nm) were used. Force spectroscopy measurements were performed using CSG30 probes from NT-MDT (k = 0.13–2 N/m, f_{res}=26–76 kHz, r_{tip}= 6 nm). The spring constant of the cantilever was determined using calibration feature from Nanoidea.[58,59] The data was processed using SPIP software from image metrology.[60]

RESULTS AND DISCUSSION

Thermal Properties of Composite Membranes

The thermal stability of the both membranes (Nafion-115/PI and Nafion-115/PI/Im) was tested by TGA at a heating rate of 10°C/min under nitrogen atmosphere. For both membranes, two weight loss stages around 330 and 450°C were observed (Table I). We did not observe changes in the thermal stability for the Nafion-115/PI membrane in comparison with Nafion-115/PI/Im and also Nafion-115/Im[51] ones. Both membranes had good thermal stability with 5% weight loss temperature of 328°C, which is attributed to the decomposition of the SO_3H groups.[4] For pure Nafion-115 5% weight loss temperature at 288°C was found. It is clearly seen that decomposition temperatures of the composed membranes were about 40°C higher than that of Nafion-115. Similar results were found in our previous works[50,51] and in Refs. 31 and 36. The temperatures of the maximum decomposition rate (T_p), as evidenced by the DTG curves, were observed for both membranes at 366 and 458°C. The thermal stability of Nafion-115/PI and Nafion-115/PI/Im membranes may be caused by fact that PI and Im are stable in Nafion-115 membrane.

FT-IR Study of Composite Membranes

In the FT-IR spectra of Nafion-115/PI and Nafion-115/PI/Im membranes, changes were observed only at the ranges of 1500–1730 cm^{-1} and 2700–3600 cm^{-1}as are presented in Figure 1.

FT-IR spectrum of Nafion-115/PI membrane showed peak at 1684 cm^{-1} shifted to higher wavenumber in comparison to pure Nafion-115 membrane (1630 cm^{-1} related to S-OH groups). Moreover, absorption bands characteristic from the asymmetric and symmetric stretching vibration of the carbonyl

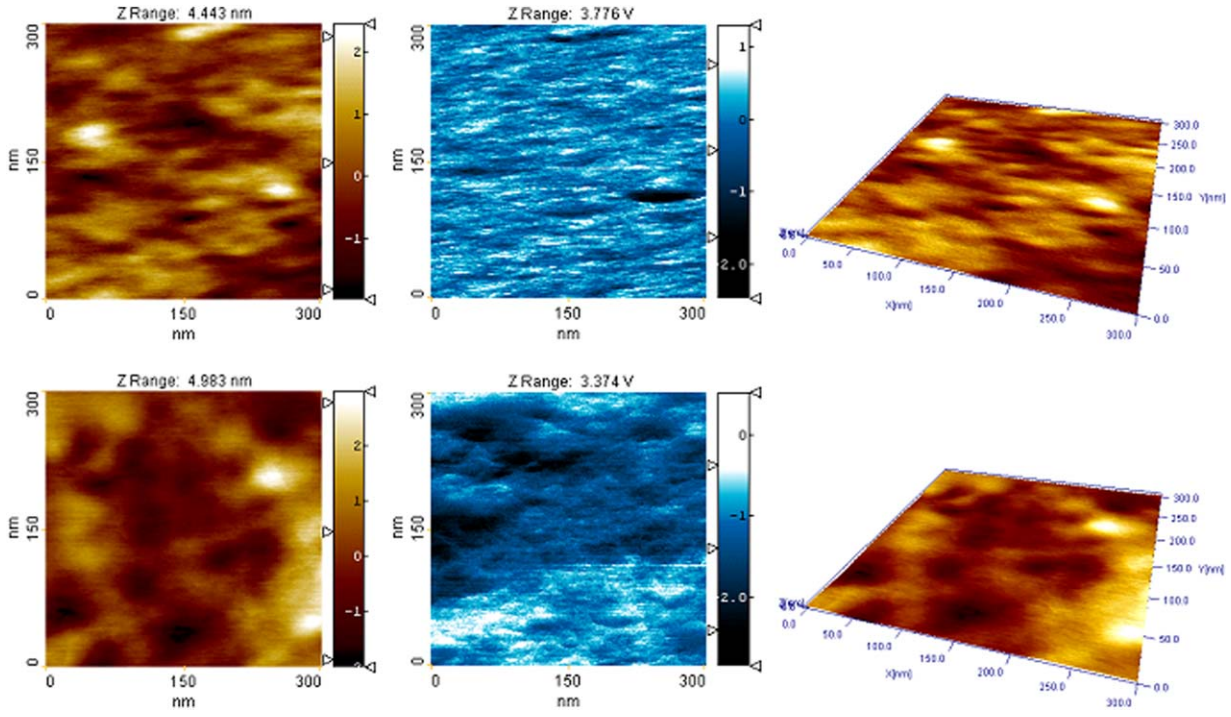

Figure 3. Topography, phase imaging, and 3D view of the topography measured with AFM for Nafion-115/PI and Nafion-115/PI/Im, from top to bottom, respectively. [Color figure can be viewed in the online issue, which is available at wileyonlinelibrary.com.]

Table III. Young Modulus for Investigated Membranes

	Young modulus (MPa)			
	Nafion-115/PI	Nafion-115/PI/Im	Nafion-115[51]	Nafion-115/Im[51]
Average value	482	616	294	116
Standard deviation	78.4	67.3	49.5	79.2

group in the imide ring of PI at 1784 and 1725 cm^{-1}, respectively,[57] in membrane are shifted to lower wavenumber (Figure 1). This is an effect of hydrogen bonding interactions between PI and Nafion-115 as schematically is presented in Figure 2.

In Nafion-115/PI/Im membrane peaks at 1689 and 1736 cm^{-1} was found which were shifted to higher wavenumber in comparison with Nafion-115/PI and Nafion-115/Im membranes as an effect of protonation of hydrogen acceptor sites (-N=C-) in Im by hydrogen atom of SO_3H group of Nafion-115 as schematically is presented in Figure 2.

Some differences were found also in the range of 2700–3600 cm^{-1}. Broad peak at about 3431 cm^{-1} of pureNafion-115 is responsible for the O-H stretch. For Nafion-115/PI and Nafion-115/PI/Im membranes shape, intensity and position of this peak was changed (Figure 1). This indicates that hydrogen bonding was created in the membrane. Similar behavior was found by Sannigrahi *et al.* for PBI gel membrane,[61] Li *et al.* for Nafion hybrid membrane[62] and in our previous work.[50,51]

Morphology of Composite Membranes

The surface morphology of both membranes was measured with AFM technique and such parameters as roughness (S_a, S_q), skewness S_{sk} (the unbalance of height distribution maximum) and kurtosis S_{ku} (the peak's width on height distribution) were calculated (Table II). Also, surface area ratio (S_{dr}) was determined, as a significant factor in terms of chemical activity.[63] The roughness of Nafion-115/PI/Im is higher than Nafion-115/PI; however, the surface area ratio is higher in case of Nafion-115/PI. It should be emphasized, that roughness of investigated samples are comparable or lower than Nafion-115 and Nafion-115-Im.[51] Surface area ratio of Nafion-115/PI/Im and Nafion-115/PI on the other hand is significantly lower than in case of previously tested materials. Nafion-115/PI, Nafion-115 and Nafion-115-Im reveal oval-like morphological features indicating some sort of existing or fixed tension in the material, while in Nafion-115/PI/Im the objects are round, and no specific direction of deformation can be pointed. Phase imaging feature reveals no significant non homogeneities in terms of the scanning tip-sample energy dissipation. In general the topography related fluctuations can be noted. It should be underlined, however, that for Nafion-115/PI/Im sample, the phase imaging features are significantly smaller than morphological ones. Also their shapes are often oval showing similarities to Nafion-115/PI sample. Figure 3 shows AFM topography and phase images obtained for both membranes.

Mechanical Properties of Composite Membranes

Mechanical properties of both composite membranes were determined using force spectroscopy technique. Obtained data revealed significantly higher values of Young modulus for Nafion-115/PI/Im and Nafion-115/PI than for Nafion-115-Im and Nafion-115 indicating an influence of performed procedure of dipping the membranes into PI or PI/Im DMA solution on mechanical properties (Table III).

The highest average value of E at about 616 MPa was found for Nafion-115/PI/Im membrane.

Water Uptake of Composite Membranes

For Nafion-115/PI and Nafion-115/PI/Im membranes the WU were detected. WU measurements were performed with aid of surface area and porosity analyzer in order to obtain the water sorption isotherms for particular membrane materials. WU values were then calculated from the equation: $WU = \frac{m_w - m_d}{m_d} \times 100$, where m_d is the mass of dry membrane whereas m_w is the total mass of dry membrane and the water absorbed at the relative pressure of about 0.9 p/p^0, according to isotherms (Figure 4).

The highest WU was found for prisitne Nafion-115 membrane (12.7%, for water activity of 0.9). Nafion-115/PI and Nafion-115/Im membranes exhibited lower value of 11.5 and 7.6%, respectively, than Nafion-115 (Table IV) which may be explained that some adsorption centers had already been occupied by incorporated membrane modifiers before the water sorption analysis was performed.

Single PEMFCs Performance Test

Polarization Curves. Electrochemical properties of constructed single PEMFCs based on Nafion-115/PI and Nafion-115/PI/Im membranes were analyzed taking into consideration the value of

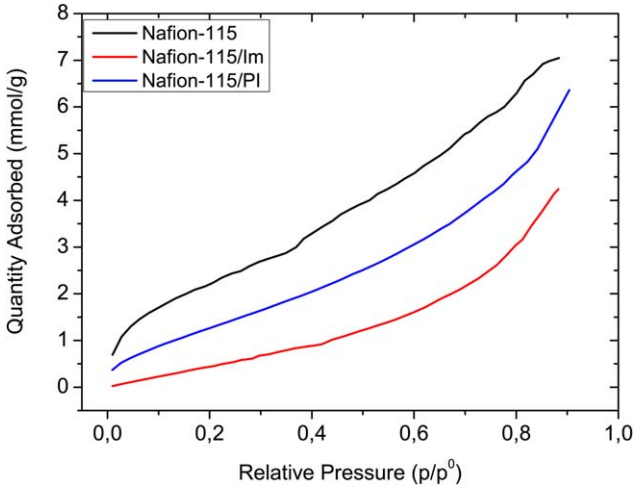

Figure 4. Water sorption isotherms for particular composite membranes and pristine Nafion. [Color figure can be viewed in the online issue, which is available at wileyonlinelibrary.com.]

Table IV. Summary of Electrochemical Properties of the Single PEMFCs at 25 and 60°C

Code	Nafion-115/PI	Nafion-115/PI/Im	Nafion-115[51]	Nafion-115/Im[51]
25/60°C				
J_{max} (mA/cm^2)	368/484	331/277	212/299	347/463
J at 0.6 V (mA/cm^2)	107/228	56/98	83/84	136/157
P_{max} (mW/cm^2)	113/171	90/92	76/95	124/140
Efficiency at P_{max} (%)	26/31	22/29	29/27	30/27
Efficiency at 0.6 V (%)	41/40	41/41	40/41	41/41
OCV (V)	0.98/0.96	0.98/0.92	0.97/0.91	0.84/0.89
σ (mS/cm)	35.3/56.2	57.8/49.6	25.8/45.9	44.4/54.1
ESA (cm^2/g)	1544	664	2465	828
Water uptake (%)	11.5	-	12.7	7.6
H_2 crossover (mole/cm^2 s)	6.04×10^{-10}	~0	~0	9.98×10^{-9}

temperature used and the presence of imidazole (Table IV). Figure 5 shows the polarization curves of both composite membranes-based PEMFCs at 25 and 60°C in comparison to single PEMFC based on Nafion-115/Im.

For Nafion-115/PI membrane, the increase of performance in case of constructed single PEMFC compared to pure Nafion-115 and Nafion-115/Im membranes was observed.[51] Moreover, for both membranes parameters at 60°C are higher than in 25°C, except OCV and efficiency at 0.6 V (Table IV). For both constructed PEMFCs the efficiency at 0.6 V was found about 41% (Table IV). For the Nafion-115/PI membrane, the highest maximum power density (P_{max}) 170 mW/cm^2, the highest open circuit voltage (OCV) of ~0.96 V and the highest value of J at 0.6 V of ~228 mA/cm^2 at 60°C compared to the other membranes was found (Figure 5 and Table IV). Electrochemical properties of Nafion-115/PI/Im single PEMFC were worse than that for Nafion-115/PI.

Electrochemical Impedance Spectroscopy. Electrochemical impedance spectroscopy (EIS) measurements of both investigated single PEMFCs at 25 and 60°C with dedicated equivalent circuit model are presented in Figure 6, while fitting parameters of the equivalent circuit are presented in Table V. EIS experiments were analyzed based on the following papers.[64,65]

The constructed single PEMFCs at 25 and 60°C exhibited semicircles in Nyquist plots. Noticeable drop in values of the real part (Z′) and the imaginary part (Z″) of the complex impedance at 60°C could be seen (Figure 6). A higher drop in Z′ along with the increase of temperature was found for Nafion-115/PI/Im than for Nafion-115/PI, while for Nafion-115/Im almost no differences were observed. In the other words, in this case, the highest drop of charge and mass transport resistance was observed for PI/Im-based single cell. The improved conductivity (σ) for PI-based membrane at 60°C was observed, whereas for Nafion-115/PI/Im a slight drop was detected. Immersion of Nafion-115 membrane in Im causes the increase of ionic conductivity in comparison to Nafion-115 membrane (44.4 mS/cm) (Table IV).

Along with the temperature increase to 60°C, the impedance module |Z| decrease in the frequency range 0.1–1 Hz was observed for both investigated membranes (Figure 6). The highest |Z| drop was found for Nafion-115/PI/Im membrane along with the increase of temperature. For both investigated single PEMFCs at 25 and 60°C, the highest value was obtained for R_2

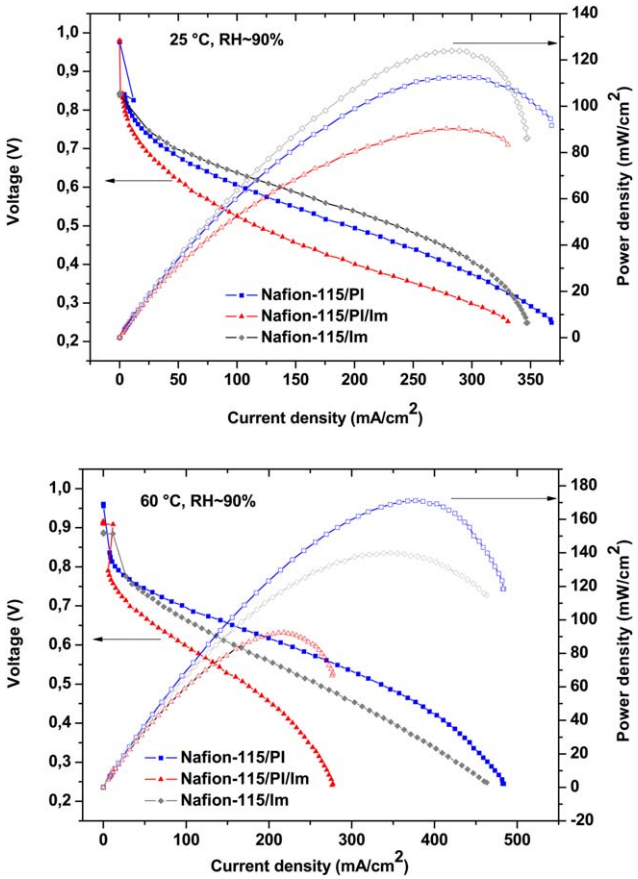

Figure 5. Polarization curves of single PEMFCs based on Nafion-115/PI and Nafion-115/PI/Im membrane and for comparison for Nafion-115/Im at 25°C and 60°C. [Color figure can be viewed in the online issue, which is available at wileyonlinelibrary.com.]

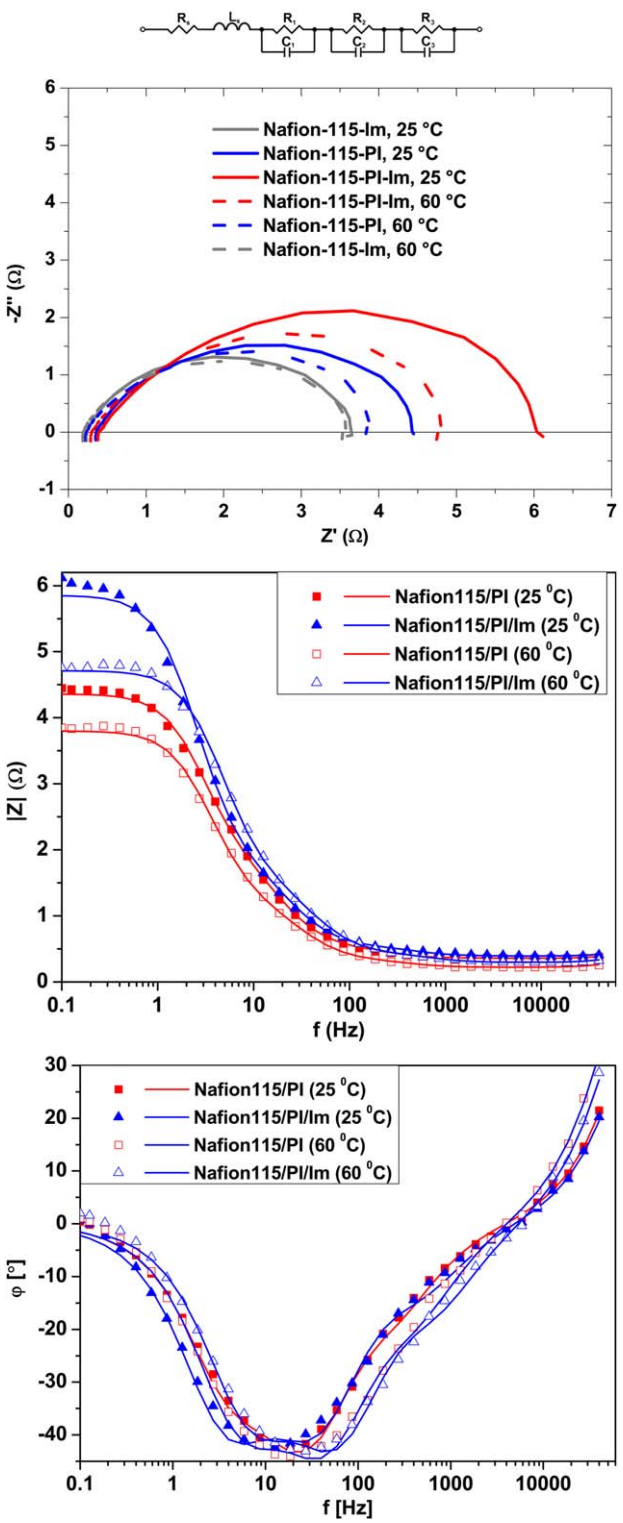

Figure 6. Impedance spectra of single PEMFCs at 25 and 60°C (calculated data: solid line: experimental data: symbols) along with equivalent circuit used for the evaluation of measured impedance spectra (R1||C1, element correspond to the rate determining processes at the anode; R2||C2, the finite diffusion element; R3||C3, element correspond to the rate determining processes at the cathode; Rs, membrane resistance and series resistance; Ls, feed line inductivity). [Color figure can be viewed in the online issue, which is available at wileyonlinelibrary.com.]

while the lowest for R_1 (Table V). Moreover, Nafion-115/PI/Im membrane exhibited the highest value of R_2 compared not only with Nafion-115/PI but also with Nafion-115/Im and Nafion-115 (Table V). Value of R_1 (at 60°C) was similar for all investigated membranes.

It has to be underlined that the equivalent model fits the measurement data very well; however, various RC elements cannot be assigned to the particular subprocesses as EIS arcs strongly overlap.

Investigations of pristine PI film reveals that it is an insulator, therefore direct application as a fuel cell membrane is impossible. EIS spectrum was recorded with aid of dielectric interface (Solartron 1296) for PI membrane in the frequency range from 40 kHz to 10^{-4} Hz with signal amplitude of 250 mV to evaluate membrane through-plane resistance. The film was placed between two gold plates and tested under STP conditions. According to the measurement data, in the given frequency range, the real part of impedance varies from 620 Ω to $1.2 \cdot \times 10^{12}$ Ω. The experiment was performed *ex-situ*; however, *in-situ* fuel cell measurements taken without dielectric interface lead to the similar conclusion. In spite of these results the addition of PI to Nafion membrane brings positive feedback in terms ionic conductivity as slight improvement of this parameter has been recorded (Table IV).

Cyclic Voltammetry. Cyclic voltametry (CV) showed some differences in H_2 adsorption/desorption peaks depending on the membrane applied. In the case of Nafion-115/PI/Im membrane, H_2 adsorption/desorption peaks were found in the range 0.1–0.3 V, while the double-layers around 0.4 V were observed. On the other hand for Nafion-115/PI membrane H_2 adsorption/desorption peaks were found in two ranges: the first at 0.1–0.3 V and the second one at 0.4–0.6 V (Figure 7).

The electrochemical surface area (ESA) of Nafion-115/PI and Nafion-115/PI/Im membranes was approximately 1544 and 664 cm^2/g, respectively, which is lower than that of the Nafion-115 membrane (2465 cm^2/g) (Table IV). The lowest value of ESA for Nafion-115/PI/Im membrane compared with Nafion-115/PI is probably caused by platinum poisoning effect due to the imidazole presence. The same effect was observed for Nafion-115/Im compared with Nafion-115.[51] The imidazole reduces the electrochemical reactions due to lower amount of available platinum in PEMFCs, but at the same time enhances the conductivity (Table IV). Similar behavior was observed for Nafion-Im membranes by Yang *et al.*[25] and in our previous work.[51] It is interesting that Nafion-115/PI membrane exhibited lowest ESA value and the highest J_{max} and conductivity than pure Nafion-115. These observations suggested that PI decreases the amount of Pt in PEMFCs similar as imidazole.

Linear Sweep Voltammetry. Linear sweep voltammetry (LSV) of Nafion-115/PI and Nafion-115/PI/Im membranes presented in Figure 8 and in Table IV showed that in the case of Nafion-115/PI membrane H_2 crossover was observed (6.04×10^{-10} mole/cm^2 s) but was lower than for Nafion-115/Im. This finding confirmed that apart from having negative

Table V. The Equivalent Circuit Parameters for All Single PEMFCs Obtained from the Fitting

Code	Nafion-115/PI	Nafion-115/PI/Im	Nafion-115[51]	Nafion-115/Im[51]
25/60°C				
χ^2 ($\times 10^{-6}$)	325/716	751/596	1163/711	426/586
R_S (Ω) Error %	0.359/0.223	0.393/0.296	0.51/0.28	0.23/0.19
	0.54/0.85	0.87/0.83	0.89/0.85	0.63/0.78
L_S (nH) Error %	551/562	561/618	440/573	624/614
	3.52/3.36	5.68/3.62	5.46/3.96	2.51/2.56
R_1 (Ω) Error %	0.127/0.088	0.125/.116	0.23/0.11	0.09/0.10
	6.99/9.47	8.17/7.24	11.3/7.74	9.70/9.92
C_1 (mF) Error %	5.221/4.697	2.731/2.157	4.90/3.76	7.16/5.08
	6.48/8.92	10.8/8.25	9.30/9.03	7.43/6.54
R_2 (Ω) Error %	2.899/2.882	4.466/3.508	3.90/3.18	2.34/2.25
	2.21/1.72	1.59/1.56	3.21/1.56	3.86/3.37
C_2 (mF) Error %	21.73/19.39	17.60/0.012	29.3/23.6	18.4/17.7
	5.22/4.34	3.86/3.96	7.88/3.83	8.31/7.80
R_3 (Ω) Error %	0.974/0.607	0.871/0.793	1.07/0.60	0.91/0.97
	6.31/6.78	6.10/5.77	10.1/6.24	9.85/7.51
C_3 (mF) Error %	10.65/10.51	8.835/5.958	14.0/12.4	9.96/7.03
	3.29/4.86	4.52/4.01	7.62/4.92	4.16/3.84

$R_1||C_1$, element correspond to the rate determining processes at the anode; $R_2||C_2$, the finite diffusion element; $R_3||C_3$, element correspond to the rate determining processes at the cathode; R_s, membrane resistance and series resistance; L_s, feed line inductivity.

influence on electrochemical properties of PI/Im-based fuel cells, PI with isopropylidene groups have also disruptive impact on the impermeability of membranes towards hydrogen crossover.

The differences in electrochemical properties of single PEMFCs observed in this work could be explained by the fact that two possible proton conducting mechanism existed depending on the kind of membrane. In the case of Nafion-115 membrane the vehicle-type mechanism (charge transport is carried out by common physical diffusion) is predominated, while in the case of Nafion-115/PI and Nafion-115/PI/Im membranes instead of vehicle-type mechanism increased also Grotthuss-type mechanism (charge transport is carried out by structure diffusion).[15,16,33,36,37,39,51] As it was mentioned previously, Im can acts as proton donor and acceptor and in our case could interaction between PI and Nafion-115. Moreover, hydrogen bonding creation between Im molecules could not be excluded as was presented in Ref. 16. However, this conclusion cannot be proven based on measurement techniques used in this work.

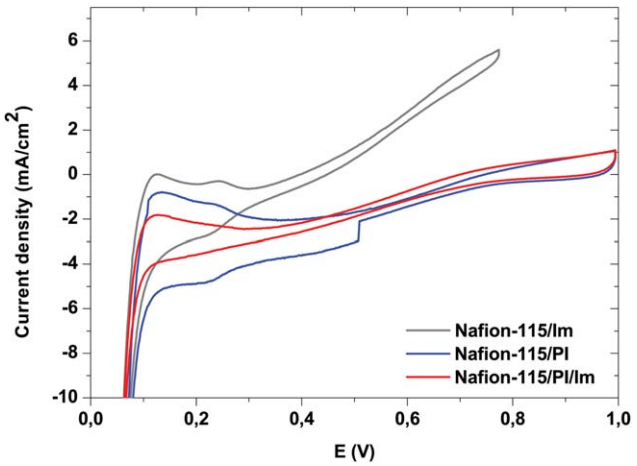

Figure 7. Cyclic voltammograms of the MEA with Nafion-115/PI, Nafion-115/PI/Im and for comparison for Nafion-115/Im. [Color figure can be viewed in the online issue, which is available at wileyonlinelibrary.com.]

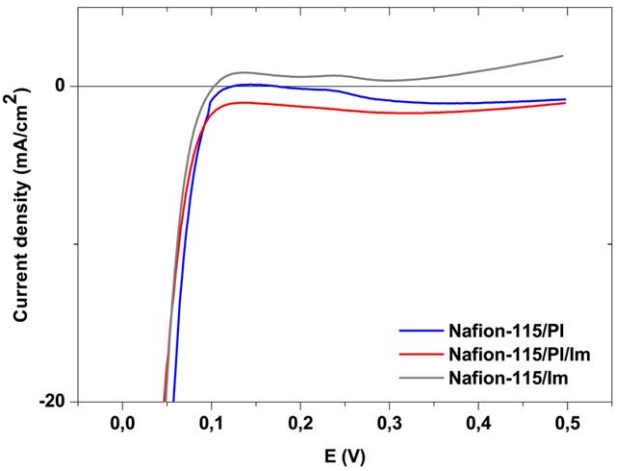

Figure 8. Linear sweep voltammetry of single PEMFCs. [Color figure can be viewed in the online issue, which is available at wileyonlinelibrary.com.]

CONCLUSION

In this work, we have studied the influence of aromatic poly(etherimide)s with isopropylidene groups on the electrochemical properties of single PEMFCs based on Nafion-115. The following conclusions can be drawn from the presented work:

1. Decomposition temperatures of the PI membranes were about 40°C higher than that of Nafion-115.
2. Single PEMFC with PI exhibited significantly better electrochemical properties at 60°C than at 25°C in comparison to other membranes investigated in this work.
3. Immersion of Nafion-115 in PI increases the current, power density and conductivity compared with Nafion-115/PI/Im and Nafion-115/Im membrane. For the Nafion-115/PI membrane the highest: P_{max} at 170 mW/cm^2, OCV of ~0.96 V, J at 0.6 V of ~228 mA/cm^2 and $\sigma \sim$ 56.2 mS/cm at 60°C were found.
4. PI increased mechanical properties of the Nafion-115 membrane as detected by force spectroscopy.
5. Apart from improving the fuel cell performance, imidazole and PI with isopropylidene groups revealed also the negative influence on electro-catalytic properties of electrodes (reduced ESA) and the impermeability of hydrogen through polymer membranes.

ACKNOWLEDGMENTS

Authors thank Mr. L. Gorecki for TGA experiments and Mr. K. Parafiniuk for preparation of membranes.

REFERENCES

1. Hickner, M. A.; Ghassemi, H.; Kim, Y. S.; Einsla, B. R.; McGrath, J. E. *Chem. Rev.* **2004**, *104*, 4587.
2. Liaw, D.-J.; Wang, K.-L.; Huang, Y.-C.; Lee, K.-R.; Lai, J.-Y.; Ha, C.-S. *Progr. Polym. Sci.* **2012**, *37*, 907.
3. Dhara, M. G.; Banerjee, S. *Progr. Polym. Sci.* **2010**, *35*, 1022.
4. Pan, H.; Pu, H.; Chang, Z.; Jin, M.; Wan, D. *Electrochim. Acta* **2010**, *55*, 8476.
5. Pu, H.; Wang, D. *Electrochim. Acta* **2006**, *51*, 5612.
6. Sakamoto, M.; Nohara, S.; Miyatake, K.; Uchida, M.; Watanabe, M.; Uchida, H. *Electrochim. Acta* **2014**, *137*, 213.
7. Li, X.; Song, Y.; Liu, Z.; Feng, P.; Liu, S.; Yu, Y.; Jiang, Z.; Liu, B. *High Perform. Polym.* **2014**, *26*, 106.
8. Gu, X.; Xu, N.; Guo, X.; Fang, J. *High Perform. Polym.* **2013**, *25*, 508.
9. Asano, N.; Aoki, M.; Suzuki, S.; Miyatake, K.; Uchida, H.; Watanabe, M. *J. Am. Chem. Soc.* **2006**, *128*, 1762.
10. Miyatake, K.; Omata, T.; Tryk, D. A.; Uchida, H.; Watanabe, M. *J. Phys. Chem. C* **2009**, *113*, 7772.
11. Fang, J.; Guo, X.; Harada, S.; Watari, T.; Tanaka, K.; Kita, H.; Okamoto, K.-I. *Macromolecules* **2002**, *35*, 9022.
12. Yamazaki, K.; Kawakami, H. *Macromolecules* **2010**, *43*, 7185.
13. Pan, H.; Zhu, X.; Jian, X. *Electrochim. Acta* **2010**, *55*, 709.
14. Dahi, A.; Fatyeyeva, K.; Langevin, D.; Chappey, C.; Rogalsky, S. P.; Tarasyuk, O. P.; Marais, S. *Electrochim. Acta* **2014**, *130*, 830.
15. Jiang, B.; Pu, H.; Pan, H.; Chang, Z.; Jin, M.; Wan, D. *Electrochim. Acta* **2014**, *132*, 457.
16. Pu, H.; Qin, Y.; Tang, L.; Teng, X.; Chang, Z. *Electrochim. Acta* **2009**, *54*, 2603.
17. Zhan, H.; Shen, P. K. *Chem. Rev.* **2012**, *112*, 2780.
18. Peighambardoust, S. J.; Rowshanzamir, S.; Amjadi, M. *Int. J. Hydrogen Energy* **2010**, *35*, 9349.
19. Sahu, A. K.; Pitchumani, S.; Sridhar, P.; Shukla, A. K. *Bull. Mater. Sci.* **2009**, *32*, 285.
20. Bose, S.; Kuila, T.; Nguyen, T. X. H.; Kim, N. H.; Lau, K.; Lee, J. H. *Progr. Polym. Sci.* **2011**, *36*, 813.
21. Asensio, J. A.; Sanchez, E. M.; Gomez-Romero, P. *Chem. Soc. Rev.* **2010**, *39*, 3210.
22. Li, Q.; Jensen, J. O.; Savinell, R. F.; Bjerrum, N. J. *Progr. Polym. Sci.* **2009**, *34*, 449.
23. Tripathi, B. P.; Shahi, V. K. *Progr. Polym. Sci.* **2011**, *36*, 945.
24. Satterfield, M. B.; Majsztrik, P. W.; Ota, H.; Benziger, J. B.; Bocarsly, A. *J. Polym Sci. Part B Polym. Phys.* **2006**, *44*, 2327.
25. Yang, C.; Costamagna, P.; Srinivasan, S.; Benziger, J.; Bocarsly, A. B. *J. Power Sources* **2001**, *103*, 1.
26. Hickner, M. A.; Ghassemi, H.; Kim, Y. S.; Einsla, B. R.; McGrath, J. E. *Chem. Rev.* **2004**, *104*, 4587.
27. Aili, D.; Hansen, M. K.; Pan, C.; Li, Q.; Christensen, E.; Jensen, J. O.; Bjerrum, N. *J. Int. J. Hydrogen Energy* **2011**, *36*, 6985.
28. Arunbabu, D.; Sannigrahi, A.; Jana, T. *J. Phys. Chem. B* **2008**, *112*, 5305.
29. Ainla, A.; Brandell, D. *Solid State Ionics* **2007**, *178*, 581.
30. Guan, Y.; Pu, H.; Pan, H.; Chang, Z.; Jin, M. *Polymer* **2010**, *51*, 5473.
31. Yang, J.; Che, Q.; Zhou, L.; He, R.; Savinell, R. F. *Electrochim. Acta* **2011**, *56*, 5940.
32. Jheng, L.-C.; Hsu, S. L.-C.; Lin, B.-Y.; Hsu, Y.-I. *J. Membr. Sci.* **2014**, *460*, 160.
33. Zuo, Z.; Fu, Y.; Manthiram, A. *Polymers* **2012**, *4*, 1627.
34. Subbaraman, R.; Ghassemi, H.; Zawodzinski, T. *Solid State Ionics* **2009**, *180*, 1143.
35. Subbaraman, R.; Ghassemi, H.; Zawodzinski, T. A. *J. Am. Chem. Soc.* **2007**, *129*, 2238.
36. Fu, Y.-Z.; Manthiram, A. *J. Electrochem. Soc.* **2007**, *154*, B8.
37. Kreuer, K. D.; Fuchs, A.; Ise, M.; Spaeth, M.; Maier, J. *Electrochim. Acta* **1998**, *43*, 1281.
38. Schechter, A.; Savinell, R. F. *Solid State Ionics* **2002**, *147*, 181.
39. Deng, W.-Q.; Molinero, V.; Goddard, W. A., III. *J. Am. Chem. Soc.* **2004**, *126*, 15644.
40. Chandan, A.; Hattenberger, M.; El-kharouf, A.; Du, S.; Dhir, A.; Self, V.; Pollet, B. G.; Ingram, A.; Bujalski, W. *J. Power Sources* **2013**, *231*, 264.

41. Wang, Y.-Z.; Chang, K.-J.; Hung, L.-F.; Ho, K.-S.; Chen, J.-P.; Hsieh, T.-H.; Chao, L. *Synth. Met.* **2014**, *188*, 21.

42. Song, M.-K.; Zhu, X.; Liu, M. *J. Power Sources* **2013**, *241*, 219.

43. Hara, R.; Endo, N.; Higa, M.; Okamoto, K.-I.; Zhang, X.; Bi, H.; Chen, S.; Hu, Z.; Chen, S. *J. Power Sources* **2014**, *247*, 932.

44. Li, X.; Chen, X.; Benicewicz, B. C. *J. Power Sources* **2013**, *243*, 796.

45. Ahn, C.-Y.; Cheon, J.-Y.; Joo, S.-H.; Kim, J. *J. Power Sources* **2013**, *222*, 477.

46. Yun, Y. S.; Bak, H.; Jin, H.-J. *Synth. Met.* **2010**, *160*, 561.

47. Martin, S.; Li, Q.; Steenberg, T.; Jensen, J. O. *J. Power Sources* **2014**, *272*, 559.

48. Taherian, R. *J. Power Sources* **2014**, *265*, 370.

49. Hyun, K.; Leeb, J. H.; Yoon, C. W.; Cho, Y.-H.; Kim, L.-H.; Kwon, Y. *Synth. Met.* **2014**, *190*, 48.

50. Malinowski, M.; Iwan, A.; Parafiniuk, K.; Gorecki, L.; Pasciak, G. *Int. J. Hydrogen Energy* **2015**, *40*, 833.

51. Iwan, A.; Malinowski, M.; Sikora, A.; Tazbir, I.; Pasciak, G. *Electrochim. Acta* **2015**, *164*, 143.

52. Ueki, T.; Watanabe, M. *Macromolecules* **2008**, *41*, 3739.

53. Li, Q.; He, R.; Jensen, J. O.; Bjerrum, N. *J. Chem. Mater.* **2003**, *15*, 4896.

54. Kreuer, K. D.; Fuchs, A.; Ise, M.; Spaeth, M.; Maier, J. *Electrochim. Acta* **1998**, *43*, 1281.

55. Schuster, M. F. H.; Meyer, W. H.; Wegner, G.; Herz, H. G.; Ise, M.; Schuster, M.; Kreuer, K. D.; Maier, J. *Solid State Ionics* **2001**, *145*, 85.

56. Herz, H. G.; Kreuer, K. D.; Maier, J.; Scharfenberger, G.; Schuster, M. F. H.; Meyer, W. H. *Electrochim. Acta* **2003**, *48*, 2165.

57. Wolinska-Grabczyk, A.; Schab-Balcerzak, E.; Grabiec, E.; Jankowski, A.; Matlengiewicz, M.; Szeluga, U.; Kubica, P. *Polym. J.* **2013**, *45*, 1202.

58. Ekwińska, M.; Rymuza, Z. *Acta Phys. Polym.* **2009**, *116*, 78.

59. Sikora, A.; Bednarz, L.; Ekwiński, G.; Ekwińska, M. *Meas. Sci. Technol.* **2014**, *25*, 044015.

60. Available at: http://www.imagemet.com/. Accessed on September 25, **2014**.

61. Sannigrahi, A.; Ghosh, S.; Maity, S.; Jana, T. *Polymer* **2011**, *52*, 4319.

62. Li, Q.; He, R.; Jensen, J. O.; Bjerrum, N. *J. Fuel Cells* **2004**, *4*, 147.

63. Available at: http://www.imagemet.com/WebHelp6/Default.htm#RoughnessParameters/Roughness_Parameters.htm. Accessed on October 14, 2014.

64. Nara, H.; Momma, T.; Osaka, T. *Electrochim. Acta* **2013**, *113*, 720.

65. Wagner, N.; Kaz, T.; Friedrich, K. A. *Electrochim. Acta* **2008**, *53*, 7475.